Journal of Environmental Management 278 (2021) 111501

Contents lists available at ScienceDirect

Journal of Environmental Management

journal homepage: http://www.elsevier.com/locate/jenvman

Research article

Compositional heterogeneity of different biochar: Effect of pyrolysis temperature and feedstocks

Shaon Kumar Das [a,b,*], Goutam Kumar Ghosh [b], R.K. Avasthe [a,**], Kanchan Sinha [c]

[a] ICAR Research Complex for NEH Region, Sikkim Centre, Gangtok, Sikkim, 737102, India
[b] Palli Siksha Bhavana, Visva Bharati, Sriniketan, Birbhum, India
[c] Indian Agricultural Statistical Research Institute, New Delhi, 110012, India

ARTICLE INFO

Keywords:
Biochar
Feedstocks
Pyrolysis temperature
Physico-chemical characterization

ABSTRACT

We have quantified the influence of different pyrolysis temperature and feedstocks types on thirty six compositional characteristics of biochar. The properties of biochar were principally influenced more by the feedstocks type than pyrolytic temperature. Higher porosity and surface area illustrated its soil structural modification and nutrient retention capacity along with their utilization for wastewater adsorbents. The total carbon content in all the biochar increased upto 10.14% with the increase in pyrolysis temperature. The produced biochar can replace the conventional fossil fuels due to their high fixed carbon. The cation exchange capacity of biochar augmented with rise in pyrolysis temperature. But the dissolved organic carbon reduced exponentially with increase in temperature. At low temperature pyrolysis the polarity index tends to increase and vice-versa. All the biochar has a potential to alleviate soil boron deficiency due to its higher concentration. Therefore, dissimilar properties of biochar can be produced by selecting the right feedstock type and standardizing specific pyrolytic temperature, depending on the necessity for environmental application in a specific crisis.

This is to certify that the research paper entitled "**Compositional heterogeneity of weed, tree and crop biomass derived biochar as affected by pyrolysis temperature and feedstocks**" authored by **Shaon Kr. Das, Goutam Kr. Ghosh, R. K. Avasthe and Kanchan Sinha** is based on the original research work and no part of the manuscript has been submitted in any other journal for publication. All the authors have reviewed the manuscript before submission in this journal. The corresponding author is responsible for ensuring that the descriptions are accurate and agreed by all authors.

1. Introduction

Biochar is nothing but charcoal like materials produced by the partial pyrolysis of residue/biomass under restricted oxygen supply (Wang et al., 2018). To pick up the environment, biochar utilization as an amendment is a catalyst for the recent global enthusiasm (Novak et al., 2016). It is not only characterized by chemical (pH, EC, CEC) and morphological (pore size, bulk density, particle density) properties but also by pyrolysis conditions (temperature and duration) and biomass type (Mukherjee and Zimmerman 2013). Biomass retention and recycling into the soil from previous crop cycle (*in-situ* cycling) or outside residue incorporation into soil (*ex-situ*) has been advocated as a significant tool (Ahmad et al., 2014). Utilizing waste crop biomass for making biochar followed by its application in soil is recognized as a better way of disposal compared with direct burning in open field (Prost et al., 2012). Preparation of biochar from locally available weeds or trees biomass helps to reduce weed population in crop field which is a serious problem in organic agriculture since use of any herbicide is not permitted (Das et al., 2016). Charring temperature plays an important role in the thermochemical conversion of biomass during biochar production (Angin, 2013; Masoumeh et al., 2019). In literature there is not mentioned any fixed temperature for production of biochar and it depends on the type of biomass/feedstocks. Due to the charring conditions and feedstocks the immense inconsistency in the physico-chemical properties of biochar is noticed (Al-Wabel et al., 2017).

During designing a specialized biochar for using in agricultural contexts, pyrolysis temperature and feedstock are the main factors to be considered (Zhao et al., 2013; Muhammad et al., 2020). Increased temperature of biochar pyrolysis increases the pH of biochar and at 400–600 °C temperature more than 80% labile fraction of carbon of the

* Corresponding author. ICAR Research Complex for NEH Region, Sikkim Centre, Gangtok, Sikkim, 737102, India.
** Corresponding author.
E-mail addresses: shaon.iari@gmail.com (S.K. Das), ravisikkim@gmail.com (R.K. Avasthe).

https://doi.org/10.1016/j.jenvman.2020.111501
Received 29 July 2020; Received in revised form 3 October 2020; Accepted 8 October 2020

biomass is transferred into recalcitrant aromatic carbon (Zhang et al., 2017). The biochars' pore volume, porosity, pore structure, and BET surface area mostly build upon charring temperature and thus high temperature charring help to develop pores *via* discharge of volatile organics (Kavitha et al., 2018). The surface area, pore volume, and mineral distribution of biochars are mainly depended on biomass and charring conditions (Lehmann and Joseph, 2015). As a result of the varying quality and end users, it is imperative to characterize different biochar properties prior to selecting an appropriate char for clear-cut application (Yargicoglu et al., 2015). It is very true that biochars physical, chemical and morphological characteristics not only depend on the charring environment but also biomass type. The major challenges for todays' biochar technology is to forecast and promise the end product quality, soil benefits, agronomic acceptability and environmental sustainability from any known biomass by any given charring technology and process conditions (Ronsse et al., 2013; Hassnen et al., 2020).

Thus, study was conducted to characterize different properties of weed, tree and crop biomass derived biochar under three different charring temperature. Chemical, physical, ultimate, proximate and carbon analysis was carried out to describe actual compositions to make the biochar ready in use. TGA and FT-IR analysis were also used to verify the internal fractures, phase transitions, porosity present in biochars surface, functional group and chemical composition. Such type of data and information will help to design and develop engineered biochar for application in agriculture, environment, industry and nanotechnology. The specific objectives were to produce and judge the physical, chemical, spectral, elemental and nutrient composition that could serve as predictors of their suitability in broader applications.

2. Materials and methods

2.1. Biomass collection and biochar preparation

Maize stalk and black gram crop biomass was collected from the ICAR-Sikkim centre research farm from previous crop harvesting. Pine needle (tree) and *Lantana camara* (weed) biomass was collected from nearby farm area jungle. The biomass was shredded to pieces of ≤6 inch and oven dried at 70 °C followed by pyrolysis into biochar production unit. Charring of all the biomass (moisture level 5%) was carried out in a portable charring kiln developed by ICAR-Sikkim centre to keep the process quick, low cost and simple. Biomass was inserted into kiln, combusted at 400, 500 and 600 °C (heating rate 10 °C min^{-1} and holding temperature 4 h) and temperature was maintained by electrically operated manual switch. After preparing they were dried at 100 °C (24 h), pulverized to fine powder, sieved through 0.2 mm and used for further analysis.

2.2. Biochar yield (%)

The percentage of different biochar yield (Y) from the method was calculated using the equation as: Yield biochar $= \frac{m\ biochar}{m\ raw} \times 100\%$ ——————— (i)Where Yield biochar = mass yield of biochar, %; m biochar = mass of biochar, kg; m raw = mass of raw biomass, kg.

The produced biochar from different biomass denoted by MSB (maize stalk), PNB (pine needles), LCB (*Lantana camara*) and BGB (black gram). The different temperature for each produced biochar denoted by subscript (B_{400}, B_{500} and B_{600})

2.3. Fourier transform infra-red and thermogravimetric analysis

Fourier-transform infrared spectroscopy (FT-IR) of different biochar samples were analyzed using a Bruker ALPHA FT-IR spectrometer over 500–4000 cm^{-1} wavenumbers for identification of various functional groups present in biochar. The biochar samples (0.1%) were mixed and ground with solid KBr in order to prepare KBr-pellet thin films for analysis. Thermogravimetric analysis (TGA) was carried out to investigate solid phase and thermal decomposition pattern of biochar under the different pyrolytic environment. We used TA instrument Q50 TG analyzer for TGA analysis. The biochar samples were programmed to heat at a rate of 20 °C min^{-1} upto 600 °C. Nitrogen gas flow was controlled at 40 mL min^{-1} inside the balance chamber and 60 mL min^{-1} inside the heating furnace. We used Platinum pans for all the TG analysis. The temperature and residual weight (%) was constantly documented to estimate the thermal decompositions of biochar.

2.4. Physical properties analysis

By core method the bulk density (BD) of biochar was estimated (Veihmeyer and Hendrickson, 1948). Particle density (PD) of biochar was measured by the water pycnometer method (Hernandez-Mena et al., 2014). Porosity (PO) of biochar sample was calculated as [1-bulk density/particle density) × 100]. Saturated water holding capacity (WHC) of biochar was analyzed by Keen Rackzowski box method (Keen and Raczkowski, 1921). The moisture content (MC) of the biochar samples were estimated gravimetrically after oven drying at 105 °C for 24 h. The BET surface area (BET) of different biochar samples was obtained using the Brunauer-Emmett-Teller (BET) method from the nitrogen adsorption-desorption isotherms with quantachrome-Autosorb iQ2 analyzer (Zhang et al., 2011). Micropore volume (MPV, <2.0 nm pore diameter) along with their surface area were calculated following the *t*-plot technique and here we plotted the amounts adsorbed on the porous biochar against the respective multilayer thickness (Hung et al., 2017). Total pore volumes (TPV) of biochar samples were estimated by converting the adsorbed quantity (g) into liquid N_2-volume (density 0.808 g mL^{-1}) at atmospheric pressure close to saturation. The average pore diameter (APD) of different biochar samples was calculated as [4 × V_t/S_{BET}] and here V_t denoted the total pore volume and S_{BET} denoted BET surface area. Here we assumed that all the pores were cylindrical, straight and not interconnected.

2.5. Chemical properties analysis

The cation exchange capacity (CEC) of the biochar samples were analyzed by ammonium acetate method (Chapman 1965). Exchangeable acidity (H^+ and Al_3^+) was determined by extracting the biochar sample with 1.0 M KCl followed by titration to the phenolpthalein end-point with 0.05 M NaOH (Farina and Channon 1991). The electrical conductivity (EC) of biochar was determined by an Utech microprocessor based pH-EC-Ion meter (1:10 biochar-water suspensions); pHw (in water) was determined at 1:10 (w/v) ratio; pHs (in salt) in 1 N KCl solution was determined at 1:10 (w/v). The more requirement of water for pH measurement of biochar was due to biochar low density and its propensity to float before it is fully imbibed. Calcium carbonate equivalent (CCE) was determined by the AOAC method (1999). The hot water estimation of boron (B) was used as per Berger and Truog (1939) with slight modification. The biochars' surface negative charge (SNC) properties were analyzed by the 'index' ion-adsorption methodology with a lithium chloride (LiCl) electrolyte (Chorover et al., 2004).

2.6. Proximate analysis

Proximate analysis was done for ash (Ash) and volatile matter (Vm) as per the American Society for Testing and Materials (ASTM) method (ASTM-E 872, 1982; ASTM-E 1755, 1995). Biochar (1.5 mg) and biomass was placed in hot oven and kept at 70 °C for 24 h. Then they were permitted to chill in a desiccator for 1 h and their weight has been taken. Analysis was done in triplicate to measure the precision of the measurement. Volatile matter content and ash content was estimated as weight loss after ignition in ceramic crucible. Thus the volatile matter (%) was estimated as loss of weight after ignition (850–900 °C and 6 min) in a ceramic crucible with a relaxed ceramic cap. Similarly the ash

(%) was estimated as loss of weight after ignition (at 750 °C and 6 h) in a ceramic crucible without ceramic cap. Finally the fixed carbon (FCc) was analyzed as [100 - (volatile matter + ash)]%.

2.7. Ultimate analysis

Ultimate or elemental analysis was done for total C, H, N and O concentration by a CHNS elementar analyzer (model: Elementar Vario Micro Cube, Germany). Finely powdered biochar was oven dried at 70 °C for 72 h. Approximately 1–2 mg biochar was kept in hot furnace at 950 °C and flushed with O_2 gas (jet injection) for rapid ignition that leads to maximum oxygen at combustion point and minimum gas utilization. The generated gaseous substances were separated by a temperature computed desorption column without peak overlap. Benzoic acid (C_6H_5COOH) and sulfanilic acid ($C_6H_7NO_3S$) were used as standard and analyzed before each elemental analysis to assess errors (±1%). Then we have determined total hydrogen (TH), total carbon (TC) and total nitrogen (TN) percentage (Enders et al., 2012). Then total oxygen (Ton) was calculated as Oxygen (%) = 100 - (C + H + N + Ash) %. The sulphur (S) percentage was also estimated by CHNS analyzer.

2.8. Carbon analysis

Dissolved organic carbon (DOC) was analyzed by batch test procedure. Biochar was added in water at 1:20 (w/v) and shaken for 3 h for preparation of water extracts as per the procedure of Dias et al. (2010) followed by filtration through a syringe and the DOC was estimated by a TOC analyser (Elementar; Vario TOC select model) provided two-stage processes involving oxidation and detection of carbon. The sample undergoes combustion at 680 °C with a platinum catalyst. The generated CO_2 was detected by non-dispersive-infrared detector. To determine the C:N ratio (CN), at first we have analyzed the carbon by Walkley-Black chromic acid wet oxidation method as described by Jackson (1973) and nitrogen by alkaline potassium permanganate method (Subbiah and Asija, 1956). The index for microbial carbon use efficiency (CUE) was estimated as ($\Lambda MBC/MBC + \Sigma CO_2\text{-}C$); where ΛMBC is change of microbial biomass carbon and ΣCO_2-C) is cumulative CO_2–C as microbial respiration.

2.9. Statistical analysis

Principal component analysis (PCA) and clustering of variables has been carried out using R programming language (R version 3.6.3). The PCA was employed for factor map & clustering of variables and quality of representation of the variables in a given principal components.

3. Result and discussion

3.1. Effect of pyrolysis temperature on biochar yield

The yield of biochar significantly varied in respect of charring temperature and feedstocks sources (Fig. 1). The yield decreased (20.69%) significantly with increase in pyrolysis temperature. The lower yield of biochar at higher charring temperature (600 °C) attributed to the emission of more gasses like CH_4, CO, CO_2 (Amonette and Jospeh, 2009) and accelerated chemical thermolysis as well as organic ingredients volatilization of feedstocks (Yuan et al., 2015). The participation of thermo-chemical cracking reactions and awfully high charring temperature accelerated the volatilization reaction which leads to minimize charcoal production by high temperature. The biochar yield was maximum at 400 °C (average of all feedstock was 32.63%) charring temperature followed by 500 °C (29.20%) and minimum at 600 °C (25.88%). Low temperature pyrolysis reduces the volatile matter losses and also strengthens the secondary char creating pyrolysis mechanism. Thus, the raise in pyrolysis temperature resulted into small production of biochar as reported by Zhang et al. (2013). The variability in biochar

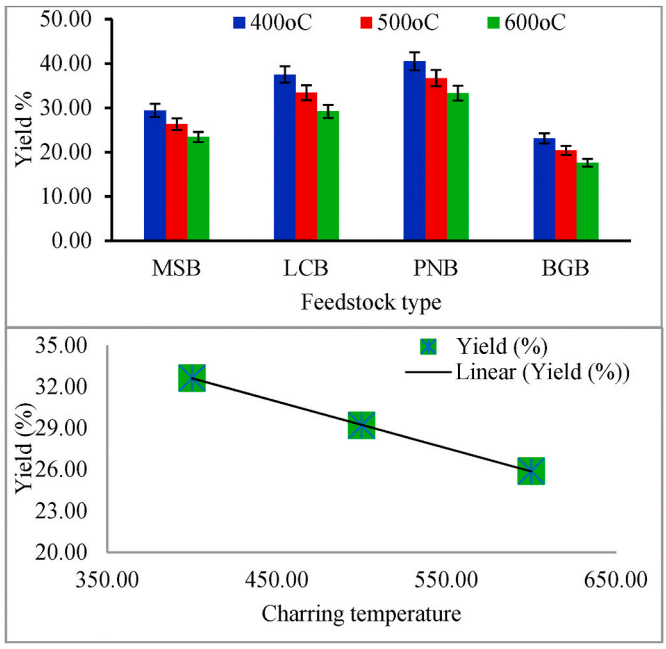

Fig. 1. a) Yield deviation of four biochar affected by charring temperature and feedstock type b) yield vs charring temperature regression equation.

yield was due to presence of varied quantity of lignocellulosic substances like lignin, cellulose and hemicelluloses in the feedstocks. The highest biochar yield (%) was recorded by PNB (40.5) followed by LCB (37.5), MSB (29.4) and lowest for BGB (23.1) at 400 °C. The maximum yield of PNB was perhaps due to utmost thermal firmness of extremely cross-linked and macromolecular organic (benzene propane) polymer lignin. In other hand the low yield of MSB and BGB might be due to presence of high amount of xylan and cellulose like polysaccharides which are comparatively rich in O_2 molecules and pyrolyzed very easily. Such findings were analogous to the TGA analysis. In a general view the woodier the feedstock there was more yield of biomass. At 600 °C there was a reduction of 20.40, 22.13, 21.62 and 23.80% yield in MSB, LCB, PNB and BGB biochar, respectively in respect to the biochar yield at 400 °C and thus maximum yield reduction was in BGB and minimum in MSB. The yield decrease in all the four biochar with increase in charring temperature may be correlated with volatile matter loss due to thermally fragmentation of volatiles into low molecular weight organic gasses and liquids by thermal decomposition and dehydration of lignocellulosic components (Chandra and Bhattacharya, 2019). Thus finally utilizing raw feedstocks having more lignin quantity may enhance the biochar production as lignin has improved thermal resistance. Further, lignin biochar having more quantity of ash might be healthier to use as potential amendments to maximize soil quality and fertility. In conclusion, both the PNB and LCB have maximum potential as biochar amendment.

3.2. Fourier transform infrared spectroscopy analysis

The FT-IR spectra of the four different biochar produced at three different temperatures represented the surface functional groups modification on the biochar during the activation and aliphatic carbon decreased but aromaticity increased (Fig. 2). The observations revealed that the concentration of different surface functional groups like phenolic, surface carboxylic, lactonic and total acidic functional groups decreased with increase in pyrolysis temperature from 400 to 600 °C. The pyrolysis of feedstocks at higher temperature produced more amounts of volatile substances and carbonaceous gasses which resulted in lower total acidic functional groups. Fig. 2 revealed that the FT-IR band intensity of the C═O/OH, -CH_n and –OH stretching decreased with increasing pyrolysis temperature due to depolymerization and

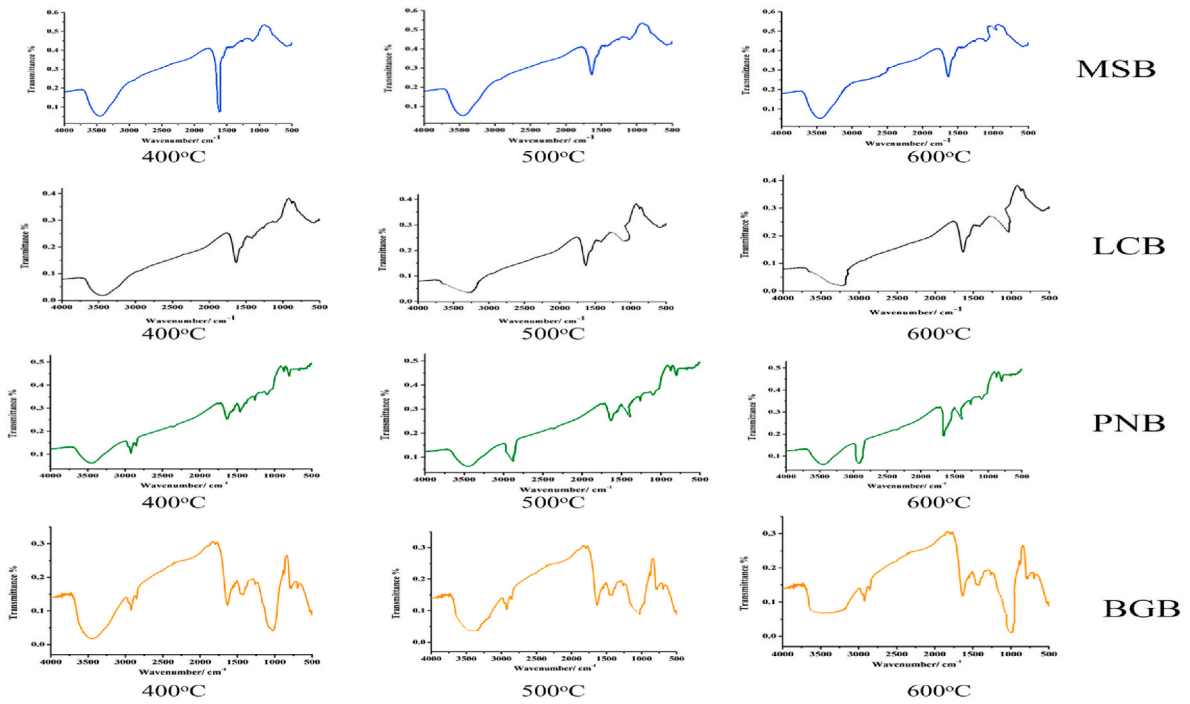

Fig. 2. Fourier-transform infrared spectroscopy (FTIR) of different produced biochar at different pyrolysis temperature.

dehydration process. Nevertheless, with increasing in pyrolysis temperature the C═C aromatic stretching band intensity enhanced due to aromatization process. Again, biochar produced at high temperature (600 °C) showed the assertive C═C aromatic carbon structure with little amount of C═O/OH or –OH groups. Hence, with increasing in pyrolysis temperature the oxygenated functional groups in all the four biochar decreased. The feedstocks type also influenced the FT-IR characteristics having slightly shifts in band position and thus wavenumber. Thus increased aromatic carbon will show more recalcitrant character and thus we can expect more carbon sequestration of biochar produced at higher temperature than lower temperature (Kolss et al., 2012). In the entire four biochars all the FT-IR graph were very similar with each other with slight changes in sharpness in peak intensity. In MSB the strong and broad peak at 3450-3500 cm^{-1} was due to due to alcoholic and phenolic O–H stretching. This peak was formed by intermolecular bonding. The band at 1550-1620 cm^{-1} was due to aromatic C═O and C═C stretching vibration (Reddy et al., 2013). After lignocellulosic (cellulose and lignin) substances condensation and decomposition the derived products were responsible for such strong and broad peak. Aliphatic C–H stretching at 2950-2850 cm^{-1} was not observed here. The different peaks observed at 590–750, 890 and 1100 cm^{-1} in all the MSB biochar produced at three different pyrolysis temperatures represented the presence of chloride and CO_3=groups. In LCB_{400} the bands at 3400-3500 cm^{-1} was due to due to alcoholic and phenolic O–H stretching which shifts (wavelength) to right side in LCB_{500} at 3250-3295 cm^{-1} and LCB_{600} at 3185-3250 cm^{-1} with lower intensity and it was due to that at higher temperature the water was disappeared in biochar and thus shifted to lower wavelength. The band at 1560-1610 cm^{-1} was due to aromatic C═O and C═C stretching vibration. The different peaks observed at 550–690, 870 and 1120 cm^{-1} in all the LCB biochar produced at three different pyrolysis temperatures represented the presence of chloride and CO_3=groups. In PNB the bands at 3450-3490 cm^{-1} was due to due to alcoholic and phenolic O–H stretching. Interestingly in PNB an aliphatic C–H stretching was observed at 2950-2850 cm^{-1} which was absent in both MSB and LCB. The reason may be that pine biomass contains oleo-resin/turpentine. The intensity of the aliphatic peak increased with increase in pyrolysis temperature. In PNB all the FT-IR graph at all the three temperature were very similar and resistance to shift in peak position which could also be due to presence of resin. In BGB the aromatic C–H peak observed was observed at 700-900 cm^{-1}, aromatic C═O and C–C stretching at 1590-1650 cm^{-1}. The peaks at wavelength 750–900 cm^{-1} was due to aromatic C–H stretching, and peak at 1580-1700 cm^{-1} was due to C–C and C–O stretching. The peak at 3450-3500 cm^{-1} was due to phenolic and alcoholic H bonds as well –COOH acid group. This peak area decreased with increase in charring temperature indicated that at higher temperature waster was evaporated and thus shrinkage of peak area at higher temperature. Similar to PNB an aliphatic peak was observed at 2950-2850 cm^{-1}. Interestingly increase in temperature the band intensity due to aliphatic O–H and C–H stretching decreases and aromatic C–Y band became more dominant. This represents that with increase in temperature water vaporize very easily and aromatization occur at higher temperature (Yuan et al., 2011). Thus it can be concluded that all the four different biochar produced at different pyrolysis temperature proved that they were carbonaceous in nature with a matrix of extremely cross linked network and the biochar produced at high charring temperature was more stable than produced at low charring temperature due to more aromatic carbon ring layers formation at higher temperature.

3.3. Thermogravimetric analysis

The Thermogravimetric analysis (TGA) curve (Fig. 3) of all the four biochar produced at different charring temperature revealed the same characteristics on the subject of mass loss (weight %) on a declining fashion with rising temperature from 0 to 600 °C. Results revealed that there was slight mass loss (weight %) from 0 to 400 °C for $MSB_{500\ \&\ 600}$ biochar and the mass loss was very fast from 401 to 600 °C. But very quick mass loss in MSB_{400} biochar was started after 300 °C. Because in our study biochar produced at lower temperature contained more moisture than higher temperature. At the initial stage the slight mass loss was due to sorbed water volatilization. Minimum amount of water was not readsorb under the ambient situation as reported by reduced water loss with increasing the biochar generation temperature. But in LCB and PNB biochar produced at all the three temperatures the trend in mass loss was more or less similar with increasing TGA temperature and it was little at early stage and faster in later stage. Finally, the BGB

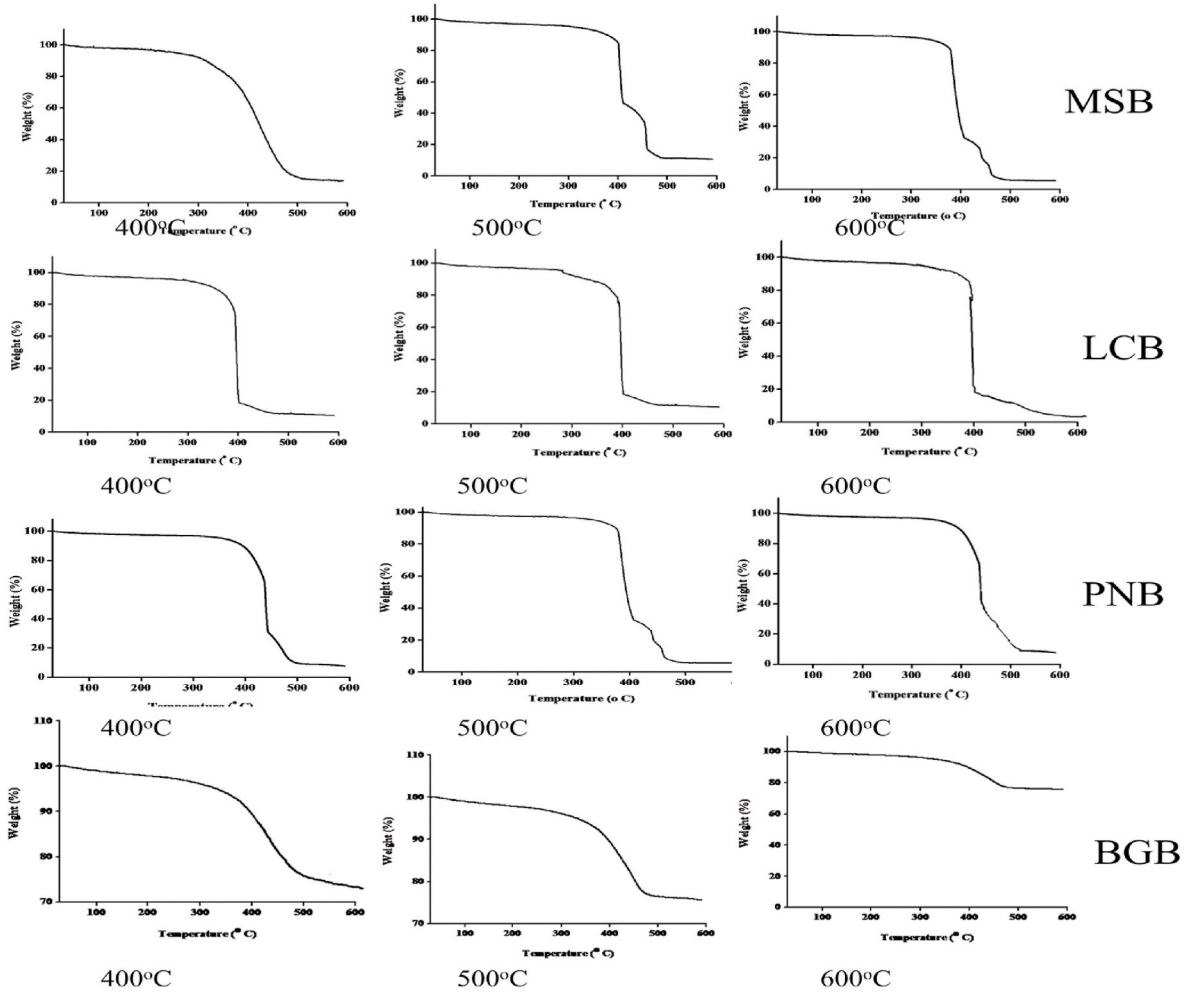

Fig. 3. Thermogravimetric analysis (TGA) of different biochar produced at different pyrolysis temperature.

biochar produced at all the three temperature showed dissimilar mass loss with increasing TGA temperature. Here, the very early stage mass loss was seen in $BGB_{400\ \&\ 500}$ and BGB_{600} showed a mass loss in later stage. The weight loss was very fast in BGB biochar because the black gram biomass is less wooly than other biochar (more woody). Thus, both the charring temperature and feedstocks significantly enhanced the mass loss under TGA analysis. In our study we have observed three different types of TGA mass loss pattern of the biochar. The mass loss from 0 to 200 $_{o}$C was due to biochars' moisture release in the form of volatilization, release of volatile matter and very loose substances attached to biochar. The TGA mass loss from 200 to 550 °C for all the four biochar type irrespective of charring temperature was due to biochars' organic matter ignition and lignocellulosic substances decomposition (Cao and Harris 2010). The mass loss in the form of organic matter and lignocellulosic substances was more at lower charring biochar then higher charring biochar and it was decreased from 42 to 56% in $biochar_{400}$ to 26-18% in $biochar_{500}$ and 3–7% in $biochar_{600}$. The mass from 550 to 600 °C was due to decomposition of calcium phosphate and calcite ($CaCO_3$) inorganic mineral (Hung et al., 2017).

3.4. Physical characterization of biochar

With increase in charring temperature the bulk density, particle density and porosity of biochar increased gradually and significantly (Table 1). They were minimum at 400 °C charring temperature followed by 500 °C and maximum at 600 °C. The highest bulk density was recorded by LCB (0.162) followed by PNB (0.153), BGB (0.142) and lowest for MSB (0.131) at 600 °C. It has already been found that woods derived biochar showed higher bulk density because of their intrinsic superior density as compared to non-woody type feedstocks. In our study the feedstocks were partially non-woody (PNB and LCB) and fully non-woody (BGB and MSB); and thus results revealed lower bulk density of biochar. The lower bulk density depicted that all the biochar were highly porus and it was confirmed by estimating the biochar porosity. Jankowska et al. (1991) found that the bulk density was enhanced by ash content of biochar which was applicable in our study where increased ash content increases the bulk density. Besides, increasing in total carbon content with increasing pyrolysis temperature was also the cause for increase in biochar bulk density. With increase in pyrolysis temperature the void space development process in biochar decrease because of raise in condensed aromatic substances concentration within sample volume and thus this resulted in increased bulk density with increase in pyrolysis temperature. The highest particle density was recorded by PNB (0.548) followed by LCB (0.516), BGB (0.483) and MSB (0.467) at 600 °C. There is also a positive correlation between the particle density and ash content of biochar suggesting that increase in ash (mineral) content increases the particle density Brown et al. (2006). With increase in pyrolysis temperature the particle density of biochar increased probably due to the calcination/shrinkage as well as lignocellulosic portion pyrolysis which results in augmented calcium oxide and aromatic carbon clusters. These statements are also applicable in our study where both the bulk density and particle density increased with increase in ash content. The highest porosity was recorded by MSB (65.90) followed by LCB (58.88), BGB (54.57) and lowest for PNB

Table 1
Physical properties of different biochar produced at heterogeneous charring temperature and feedstocks sources.

Feedstock	Temp (°C)	Bulk density (Mg m^{-3})	Particle density (Mg m^{-3})	Porosity (%)	Saturated water holding capacity SWHC (%)	BET surface area (m^2 g^{-1})	Moisture content (%)	Average pore diameter (nm)	Micropore volume (x 10^{-6} cm^3 g^{-1})	Total pore volume (cm^3 g^{-1})
MSB	400	0.12	0.35	60.20	690.45	12.90	15.62	2.97	60	2.43
	500	0.12	0.37	62.70	713.62	23.20	10.90	2.71	262	3.13
	600	0.13	0.46	65.90	701.56	43.90	7.28	3.47	465	3.53
LCB	400	0.15	0.40	53.18	576.37	12.70	12.37	2.76	53	2.89
	500	0.15	0.42	55.68	602.95	22.10	8.30	2.45	255	3.59
	600	0.16	0.51	58.88	589.46	41.40	6.26	3.12	458	3.99
PNB	400	0.14	0.43	46.96	542.39	12.50	10.36	2.35	46	1.62
	500	0.14	0.45	49.46	567.63	21.80	6.60	2.01	249	2.32
	600	0.15	0.54	52.66	553.91	40.20	4.48	2.74	452	2.72
BGB	400	0.13	0.37	48.87	557.61	12.10	11.61	3.61	48	1.37
	500	0.13	0.39	51.37	679.56	20.40	7.80	3.04	251	2.07
	600	0.14	0.48	54.57	610.59	38.90	5.62	3.96	454	2.47
Results of principal components analysis (PCA) of physical properties of different biochar										
Principal components		PC-1	PC-2	PC-3	PC-4					
Eigen value[a] variance		4.21	2.15	1.91	1.08					
Per cent cumulative		42.19	21.52	19.19	10.81					
Variance percentage		42.19	63.71	82.90	93.72					
Eigen vectors[b]										
Y		-.50	**.74**	-.12	.30					
BD		-.09	.34	**.91**	-.08					
PD		.60	**.69**	-.18	-.27					
PO		.05	.14	**.97**	-.05					
WHC		.26	**-.66**	.23	**.57**					
BET		**.96**	.20	-.05	-.09					
MC		**.96**	-.07	.05	.17					
APD		.54	-.60	.10	-.44					
MPV		**.95**	.18	-.05	-.05					
TPV		.67	.27	.01	**.57**					

* All data were mean of three replicates; **.
[a] Eigen values (>1) corresponds to the PCs were considered.
[b] Boldface factor loadings were considered highly weighted (>0.40).

(52.66). The porosity of all the biochar was maximum at 600 °C because of faster lignin decomposition and speedy discharge of gasses like CH_4 and H_2 at higher pyrolysis temperature. Besides, expanding in biochar porosity due to increased pyrolysis temperature could be justified by the fact that at higher temperature the volatiles are removed from the pores and physico-chemical condensation of remaining skeletal configuration (Brewer et al., 2011). But with increase in pyrolysis temperature the saturated water holding capacity (SWHC) of biochar increased from 400 °C to 500 °C and then again decreased drastically at 600 °C significantly. Thus, SWHC was low at 400 °C charring temperature followed by 600 °C and high at 500 °C. The highest SWHC was recorded in MSB (713.62) followed by BGB (679.56), LCB (602.95) and PNB (567.63) at 500 °C. Actually different polar functional groups are present on surfaces of biochar and perform as H_2O molecules adsorption point to assist the creation of H_2O clusters on the C-surfaces. Depending on feedstocks type and pyrolysis temperature, the tar generation and various hydrophilic groups in liquid attained a peak at 500 °C due to thermochemical lignocellulosic component decomposition (Amonette and Jospeh, 2009). At higher pyrolysis temperature most of the volatile carbon (aliphatic hydrophilic group) was lost and such type of hydrophilic group was not able to develop under low temperature pyrolysis. This resulted in repellence of H_2O molecules in biochar sample produced at lower pyrolysis temperature (<500 °C) causing poor saturated water holding capacity (Keiluweit et al., 2010). The moisture content decreased with increase in charring temperature and it high at 400 °C charring temperature and low at 600 °C. At 600 °C the moisture content was recorded by MSB (7.28), LCB (6.26), BGB (5.62) and lowest for PNB (4.48) at all charring temperature. The decrease in moisture content was due to break down of hydrogen bond which promotes evaporation of water from biochar. Biochar having poor in moisture content does not hamper the adsorptive capacity and represent it commercially feasible (Van Oss, 1990). With increase in charring temperature the BET surface area, micro pore volume and total pore volume of biochar increased significantly. At 600 °C the highest BET surface area was 43.9 for MSB, 41.4 for LCB, 40.2 for PNB and 38.9 for BGB. Results revealed that the moderate BET surface area of all the biochar might be due to alkaline and alkaline earth metal existence which may perhaps minimize BET surface area by means of pores blockage. Besides, the shrinkage in pore space of biochar may result to minimize BET surface area at high temperature (Gai et al., 2014). The highest micro pore volume was recorded for LCB (3.99), MSB (3.53), PNB (2.72) and BGB (2.47) at 600 °C. With increase in pyrolysis temperature from 400 to 600 °C the hemicellulose and many organic substances ruptured and thus produced huge pores (micro) inside the biochar. The highest total pore volume was recorded by LCB biochar followed by MSB, PNB and lowest for BGB biochar at all pyrolysis temperature. Mukome and Parikh (2016) found a positive correlation between BET surface area and charring temperature for many biochar due to the fact that huge pores are created d at high temperature. The aromaticity as well as calcination process will be enhanced by increased pyrolysis temperature in all the biochar due to creation of huge micro- and meso-pores and thereby helps to create more BET surface area. The average pore diameter was low at 500 °C charring temperature followed by 400 °C and high at 600 °C. The highest average pore diameter was recorded by BGB (3.96) followed by MSB (3.47), LCB (3.12) and lowest for PNB (2.74) at all charring temperature representing a meso- and macro-porous configuration. The higher size of all the biochar pores pointed out their utilization for wastewater adsorbents. The micropore volume and total pore volume increased with increase in charring temperature. Micropore volume was maximum in MSB followed by LCB, BGB and minimum in PNB. But total pore volume was more in LCB and low in BGB. At higher pyrolysis temperature all the micropores within the biochar converted into wider

in size by destroying adjacent pores wall and thus enlarged pores size by raising micro and total pore volume. The biochars' pore volume and pore structure mostly build upon charring temperature and thus high temperature charring help to develop pores via discharge of volatile organics (Kavitha et al., 2018). Furthermore, the decomposition of lignocellulosic components and vascular bundles (channel structure) development at the time of pyrolysis might increase in BET surface area and pore volume (Kim et al., 2013).

3.5. Chemical characterization of biochar

Table 2 revealed that the cation exchange capacity (CEC) of biochar augmented with rise in pyrolysis temperature. At 600 °C the CEC (cmol P^+ kg^{-1}) was more in MSB (55.46) followed by BGB (49.64), LCB (39.48) and lowest in PNB (37.56). The CEC varied moderately amongst various biochar created from dissimilar biomass and largely with temperature. The CEC is correlated with cations like Ca, Mg and K. Such variation in CEC among the biochar might be due to presence of different quantity of cations in different feedstocks. Besides, increase in CEC with increase in temperature was associated with the augmentation in mineral nutrients, pH and EC. The charge density of biochar and plenty of exchangeable ions in aqueous phase mainly control the CEC. Thus, biochars' negatively charged sites augmented with increase in biochar pH and allowed it to grip cationic base via electrostatic mechanism and raise their exchangeability with alternative ions in the soil. In addition, the quantity of nutrients ion augmented in aqueous phase with rise in biochar EC and accordingly exchange capability of the biochar. The high CEC of biochar is good for soil health and able to increase available plants nutrients which can increase crop production during their application in soil. The Principal component analysis (PCA) also explained to some extent positive relationship of CEC with EC and pH. The exchangeable acidity, surface negative charge and sodium content of the four different biochar decreased significantly with increase in charring temperature. Exchangeable acidity was maximum in MSB (42.45) followed by BGB (36.75), LCB (29.43) and lowest for PNB (26.75) at 400 °C. The exchangeable acidity of all the biochar was higher in range and it might be due to small surface alkalinity and more surface acidity. The exchangeable acidity decreases with increase in temperature due to increase in pHs and pHw value. At low temperature (400 °C) the exchangeable acidity of biochar was high and it could be due to presence of more amounts of acidic-carboxylic and -phenolic functional groups which was authenticated by the FT-IR analysis (Fig. 2). At 400 °C the highest surface negative charge was recorded by MSB (1.4) followed by LCB (1.1), PNB (0.9) and lowest for BGB (0.7). With increase in pyrolysis temperature the surface negative charges decreased and it was reported that low surface negative charges of biochar have protective ability for plants when applied in soil. With increase in charring temperature majority of the –COOH and –OH functional groups of biochar is reduced and thereby causes a noteworthy damage of surface negative charge. The hydrogen-bond has ability to reduce the surface negative charge while the oxygen bearing functional group may raise it. The sodium content was recorded highest in MSB (362.5) followed by BGB (332.6), LCB (315.8) and lowest for PNB (298.3). Its concentration reduced with rise in pyrolysis temperature and it can be attributed to volatile matter loss and crystalline elements development. This sodium is not an important element for crop growth and development. But it may create problem during its application in saline/alkaline soil which will cause coagulation in soil structure by clay dispersion mechanism. The electrical conductivity (EC), pHw, pHs, $CaCO_3$ equivalent (CCE), Se, boron and Cr of all the four biochar was low at 400 °C followed by 500 °C and maximum at 600 °C charring temperature. With increase in pyrolysis temperature their values increased gradually. At 600 °C highest EC was recorded by PNB (2.98) followed by MSB (1.17), BGB (1.05) and LCB (0.86). The increase in EC with increase in pyrolysis

Table 2
Chemical properties of biochar produced at heterogeneous charring temperature and feedstocks sources.

Feedstock	Temp (°C)	CEC (cmol P^+ kg^{-1})	Exchangeable acidity (cmolc kg^{-1})	EC (ds m^{-1})	pH_w	pH_s	$CaCO_3$ equivalent (CCE)	Surface negative Charge (mmol/g)	Se (mg kg^{-1})	Boron (mg kg^{-1})	Cr (mg kg^{-1})	Sodium (mg Na kg^{-1})
MSB	400	38.56	42.45	0.77	8.58	7.19	30.87	1.40	0.05	0.79	0.01	362.50
	500	47.60	35.73	0.97	9.38	8.07	36.56	0.90	0.06	1.29	0.01	341.50
	600	55.46	27.72	1.17	10.51	8.57	38.67	0.70	0.06	1.41	0.01	320.10
LCB	400	31.85	29.43	0.46	8.23	7.12	26.06	1.10	0.09	0.49	0.02	315.80
	500	33.6	24.52	0.73	9.03	8.02	31.67	0.90	0.09	0.88	0.02	291.20
	600	39.48	19.61	0.86	10.15	8.09	32.86	0.60	0.10	0.99	0.02	273.50
PNB	400	29.48	26.75	2.58	8.11	7.02	23.66	0.90	0.10	0.62	0.02	298.30
	500	32.20	22.46	2.84	8.91	7.73	29.56	0.70	0.10	0.69	0.02	277.80
	600	37.56	17.76	2.98	9.98	7.93	30.46	0.60	0.10	0.78	0.02	257.30
BGB	400	36.61	36.75	0.75	8.41	7.37	27.76	0.70	0.07	0.86	0.00	332.60
	500	42.70	28.64	0.96	9.21	7.96	33.62	0.60	0.07	0.97	0.00	312.30
	600	49.64	21.28	1.05	10.32	8.26	34.56	0.50	0.07	1.18	0.01	290.50
Results of principal components analysis (PCA) of chemical properties of different biochar												
Principal components			PC-1	PC-2								
Eigen value[a] variance			4.69	3.65								
Per cent cumulative			42.72	33.24								
Variance percentage			42.72	75.97								
Eigen vectors[b]												
CEC			**.94**	.18								
EA			**.97**	.11								
EC			-.53	-.49								
pHw			-.61	.72								
pHs			-.56	.78								
CCE			-.16	**.93**								
SNC			.74	-.29								
SE			-.29	-.30								
B			-.00	**.86**								
CR			-.61	-.55								
S			**.91**	.32								

* All data were mean of three replicates; **.
[a] Eigen values (>1) corresponds to the PCs were considered.
[b] Boldface factor loadings were considered highly weighted (>0.40).

temperature could be due to volatile matter loss from feedstocks at the time of carbonization which results in deposition of such minerals in inert ash fraction (Cantrell et al., 2012). The EC represents the entire amount of water soluble ions exist in biochar sample. It has detrimental effect on crop growth (nutrients unsteadiness and reduced water uptake) when present in larger concentration. All the biochar in this experiment showed comparatively small EC ($<$4.0 dS m^{-1}). Normally, $\geq$4.0 dS m^{-1} EC represents saline soil. Thus the low EC containing all the biochar in this study could be applied in soil and they should not have noteworthy negative role on salinity. At 600 °C the pHw was more in MSB (10.51) followed by BGB (10.32), LCB (10.15) and PNB (9.98). The highest pHw was recorded by MSB and lowest for PNB. At 600 °C the pHs was more in MSB (8.57) followed by BGB (8.26), LCB (8.09) and PNB (7.93). The values of pHw were more (strongly alkaline) than the values of pHs (slightly alkaline). In KCl (1.0 M) solution the biochar pH is more than 1 pH unit lower and it pointed out considerable reserve acidity on KCl exchangeable groups. With increase in pyrolysis temperature the pH of the biochar tends to be alkaline. Acid functional group loss/reduction and alkaline cationic elements withholding was responsible for such tendency of biochar. Besides, aromatic carbon content increased during the high temperature pyrolysis which results in pH increase in different biochar as revealed by FTIR spectra. Moreover, high temperature pyrolysis influenced the CO_3^{-2} mineral phase development process which also caused alkaline (>7.0) biochar pH (Karim et al., 2019). Overall, the alkaline pH of the biochar was due to inorganic components and organic functional groups formation at higher pyrolysis temperature (Fidel et al., 2013). Thus, the interconversion of inorganic minerals and organic functional groups present in the biochar will decide its pH. The two negatively charged –COO^- and –O^- anions (recognized in FT-IR) of biochar were participated to buffer the acidic reaction and contributed to alkaline pH of biochar via merging of such groups with H^+. Besides, among the inorganic fractions the main alkaline anions CO_3^{-2} and HCO_3^- were liable for higher biochar pHw. For that reason, the high temperature pyrolyzed biochar application may be practical to raise the acidic soil pH having highly contaminated with aluminum and iron. The highest CCE was recorded by MSB (38.67) and lowest for PNB (30.46). The role of biochar to act as a liming agent for short term effect was due to presence of ash content and long term effect was due to its oxygen containing functional groups. At the time of high temperature induced biochar production the basic cations (Ca^{+2} and Mg^{+2}) have a tendency to convert into their oxides, hydroxides and carbonates and thus accelerated the CCE of biochar. Similarly, highest selenium (Se) content was found in PNB followed by LCB, BGB and lowest for MSB. The highest boron (B) content was in MSB (1.41) followed by BGB (1.18), LCB (0.99) and lowest in PNB (0.78). Results revealed that all the feedstock derived biochar contained high concentration of plant available micronutrients boron and thus application of biochar has a potential to alleviate soil boron deficiency. Chromium (Cr) content was maximum in PNB (0.028) followed by LCB (0.025), MSB (0.015) and minimum in BGB (0.011). Apart from micronutrient boron some negligible amount of heavy metals Se and Cr were also present in all the biochar. Nevertheless, such type of heavy metal concentration was far lower than their permissible toxicity limits in soil.

3.6. Ultimate analysis

With increase in charring temperature the total nitrogen, hydrogen and oxygen content of biochar decreased significantly (Table 3). They were low at 600 °C charring temperature followed by 500 °C and high at 400 °C. At 400 °C highest total hydrogen was more in MSB biochar (3.97) followed by BGB (3.57), LCB (3.07) and PNB biochar (2.56). The highest total oxygen content was recorded by PNB (24.47) followed by

Table 3
Ultimate-, proximate-analysis and carbon content of different biochar produced at heterogeneous charring temperature and feedstocks sources.

Feedstock	Temp (°C)	Total nitrogen (%)	Total hydrogen (%)	Total oxygen (%)	Total carbon (%)	Polarity index	Ash wt (%)	Volatile matter (%)	Fixed carbon content (%)	Sulphur (%)	Dissolved organic carbon (g kg^{-1})	C:N ratio	Index for microbial C-use efficiency
MSB	400	1.39	3.97	20.64	58.80	0.42	15.2	26.56	45.56	0.08	0.75	79	0.53
	500	1.17	3.56	13.67	61.90	0.28	19.7	20.67	48.13	0.07	0.69	85	0.49
	600	0.99	3.27	6.84	65.50	0.15	23.4	17.81	49.56	0.09	0.61	87	0.41
LCB	400	1.01	3.07	14.52	69.80	0.25	11.6	28.81	52.61	0.00	0.61	91	0.95
	500	0.86	2.69	10.25	70.50	0.18	15.7	22.56	55.61	0.00	0.55	92	0.85
	600	0.61	2.39	2.70	74.10	0.07	20.2	19.48	57.67	0.00	0.46	99	0.74
PNB	400	0.97	2.56	24.47	61.70	0.44	10.3	31.46	47.73	0.05	0.67	97	0.91
	500	0.78	2.13	17.79	65.80	0.30	13.5	27.62	50.83	0.04	0.61	100	0.81
	600	0.57	1.89	12.44	68.40	0.21	16.7	24.53	52.56	0.06	0.53	105	0.85
BGB	400	1.42	3.57	22.01	53.30	0.48	19.7	28.18	39.56	0.07	0.79	71	0.43
	500	1.24	3.14	15.62	56.70	0.33	23.3	23.56	40.73	0.06	0.72	72	0.40
	600	1.02	2.88	9.30	60.30	0.202	26.5	20.61	42.29	0.08	0.63	79	0.38

Results of principal components analysis (PCA) of ultimate-, proximate-analysis and carbon content of different biochar

Principal components	PC-1	PC-2	PC-3
Eigen value[a] variance	5.31	3.07	1.12
Per cent cumulative	48.33	27.99	10.23
Variance percentage	48.33	76.32	86.56
Eigen vectors[b]			
TN	.78	-.01	-.08
TH	.77	-.10	-.39
Ton	.50	**.84**	.08
TC	**-.92**	-.18	-.22
Ash	.34	**-.85**	.02
Vm	.14	**.96**	.01
FCc	**-.92**	-.08	-.20
S	.68	-.38	.35
DOC	**.89**	.35	-.06
CN	-.35	.02	**.85**
CUE	-.77	.60	-.05

* All data were mean of three replicates; **.
[a] Eigen values (>1) corresponds to the PCs were considered.
[b] Boldface factor loadings were considered highly weighted (>0.40).

BGB (22.01), MSB (20.64) and lowest for LCB (14.52) at 400 °C. During pyrolysis procedure the decrease in oxygen and hydrogen concentration in all the biochar was due to loss of carbon dioxide, carbon monoxide, water and hydrocarbon via syngas (Gai et al., 2014). At 400 °C highest total nitrogen was in BGB (1.42) followed by MSB (1.39), LCB (1.01) and PNB (0.97). The reduction in nitrogen concentration at low temperature pyrolysis was due to loss of various forms of nitrogen (NO_3–N, NH_4–N) in R–NH_2 (amino) functional group (2800-3000 cm^{-1}) as well as organic matter volatilization and at high temperature due to –C_5H_5N (pyridine) group (1550-1600 cm^{-1}) which was confirmed by FT-IR spectra in Fig. 2 (Khanmohammadi et al., 2015). Nature of feedstocks also enhanced the composition of biochar. But interestingly, the total carbon content of biochar increased with increase in charring temperature. The total carbon was low at 400 °C pyrolysis temperature followed by 500 °C and high at 600 °C. At 600 °C the total carbon was more in LCB (74.1) followed by PNB (68.4), MSB (65.5) and BGB (60.3). In general, increasing carbon content with increasing in pyrolysis temperature in all the biochar was due to aromatic carbon structure formation and enhanced carbonization rate. Nevertheless, rise in carbon content with increasing pyrolysis temperature in al the biochar might be attributed to thermochemical carbon-hydrogen and carbon-carbon breakage due to prolonged thermal contact and stable aromatic hydrocarbons formation; and enhanced loss of different long chain aliphatic member (hemolytic dissociation) which was confirmed by FT-IR wherein the peaks representing existence of strengthen aromatic hydrocarbon. The carbon obtained from all the biochar can be used for purification and adsorption purpose as it contained very small amount of sulphur. A van Krevelen diagram (H/C and O/C ratios) for all the feedstock derived biochar produced at 400, 500 and 600 °C has been presented in Fig. 4 using the data in Table 3 for estimation of recalcitrance and aromaticity. In general, a biochar is called more stable if its molar O/C ratio is low and C/N ratio is more. Interestingly, in this study the molar O/C ratio reduced with increasing pyrolysis temperature for all the biochar pointing out the formation of more stable biochar. Besides, lower molar H/C ratio at high pyrolytic temperature represented that the all the biochar were more aromatic in nature with more stability. Such more stability of biochar at higher temperature might be due to demethylation, dehydration and alkalization process (Cely et al., 2015). Additionally, the degree of oxidation as well as stability of a biochar also depends on atomic O/C and H/C ratios. The van Krevelen diagram representing the molar atomic ratio variation as a function of biomass nature and pyrolytic temperature; and with rise in pyrolytic temperature the molar ratio of all the biochar reduced. Such reduced molar ratio was due to high degree of carbonization and loss of polar group which form huge amount of stable aromatic structure (Liu et al., 2014). The O/C ration was higher in BGB (0.41) biochar followed by PNB (0.40), MSB (0.35) and lowest in LCB (0.21). The atomic O/C ratio was more at 400 °C than at 600 °C due to presence of more ketonic, carboxylic and hydroxyl groups at lower pyrolysis temperature (Li and Chen 2018). The H/C ration was higher in MSB (0.68) biochar followed by BGB (0.67), LCB (0.44) and lowest in PNB (0.41). The atomic H/C ratio was more at 400 °C than at 600 °C due to existence of low energy hydrogen-carbon bonds (biodegradable) and thus it could be simply used by soil microbial population. The atomic H/C ratio was low at 600 °C pyrolysis temperature due to formation of aromatic structure in biochar which showed recalcitrant behaviour and thus resistant to degradation by soil microbes during its application in soil. Thus, the lower atomic O/C and H/C ratio depicted that all the biochar were more recalcitrant and aromatic in nature at higher temperature and will be stable in soil for longer period of time. Such high mean residence time of biochar at 600 °C will make it appropriate for decrease in GHGs emission, increase in soil carbon sequestration, enhanced controlled release fertilizer and soil microbes resistant when dumped in environment (Case et al., 2014). Finally, low atomic O/C and H/C ratio of biochar at high pyrolysis temperature is always acceptable and reflects favourable as well as better fuel quality than low temperature biochar. Likewise, the polarity index [(O + N)/C] of the biochar was maximum in BGB (0.48) followed PNB (0.44), MSB (0.42) and LCB (0.25) by at 400 °C. At low temperature pyrolysis (400 °C) the polarity index tends to increase and vice-versa. This depicted that biochar produced under low temperature results in more surface polar functional group and it does not depend on feedstocks type.

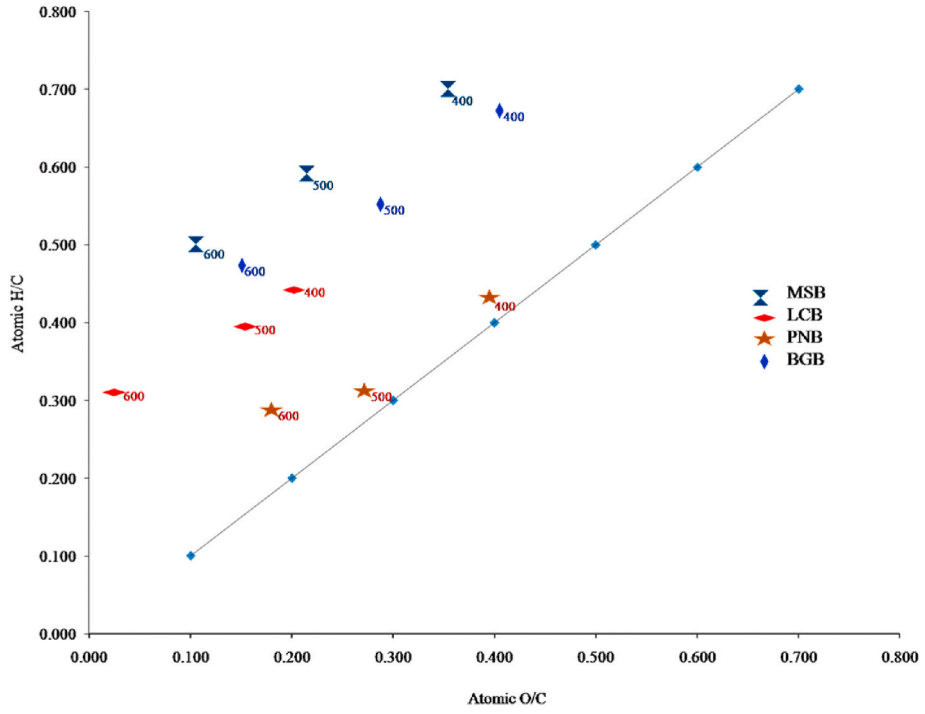

Fig. 4. van Krevelen diagram (H/C and O/C ratios) for MSB, LCB, PNB and BGB produced at 400, 500 and 600 °C.

3.7. Proximate properties

With increase in pyrolysis temperature the ash content and fixed carbon content of biochar increased significantly (Table 3). Such enhancement in ash content and fixed carbon with rise in pyrolysis temperature was mentioned for various biochar resultants from different agriculture waste by Rafiq et al., (2016). Actually the non-vulnerable part in a biochar is ash and fixed carbon which remain stable with increase in pyrolysis temperature. At 600 °C the ash was more in BGB (26.5) followed by MSB (23.4), LCB (20.2) and PNB (16.7). At high pyrolysis temperature the ash content will be more due to liberation of different organic volatile compounds like methane along with carbon monoxide, carbon dioxide and hydrogen during pyrolysis process. The highest fixed carbon was recorded by LCB biochar (57.67) followed PNB (52.56), MSB (49.56) and lowest for BG (42.29) at 600 °C. The ash content increased with increase in pyrolysis temperature between 400 and 600 °C was due to increase in the concentration of various minerals (silicon) along with volatilization of lignin, cellulose and hemicellulose substances (Rafiq et al., 2016). The increase in fixed carbon was also related to the decrease in O/C and H/C ratio along with augmentation in aromatic recalcitrant carbon in the biochar (Wu et al., 2012). At 600 °C pyrolysis temperature all the biochar contained more amounts of ash (16.7–26.5%) and therefore resulting in higher heating value (12.07–19.15 MJ kg^{-1}) than the biochar produced at 400 °C (lower heating value). It must be mentioned that total nitrogen in all the biochar were higher in range than most of energy crops (<1.0%). Notably, the fuel-bound ash/nitrogen will contribute to NO_x along with particulates emission from its direct ignition in case of highly developed air pollution management system is not established during feedstock to energy conversion. But as the sulphur content is very low in most of the biochar a little chance for sulphur oxides (SOx) emissions from its direct combustion. But the volatile matter content decreased with increase in charring temperature and it was high at 400 °C and low at 600 °C. At 400 °C the highest volatile matter was in PNB (31.46) followed by LCB (28.81), BGB (28.18) and MSB (25.56). With increase in pyrolysis temperature the vulnerable volatile matter fractions start to decompose, because of thermochemical transformation, resulting in degradation of pyrolytic volatile substances towards low molecular weight gasses (Kim et al., 2012). Such type of gasses can easily run away from the feedstocks material via syngas (Rafiq et al., 2016). With rise in pyrolysis temperature the volatile fractions undergoes further cracking and produced low molecular weight gasses and liquids rather than solid biochar. In most cases, biochar having more amount of volatile matter assist crop growth and development due to presence of easily decomposable organics in larger quantity. In such situation, biochar produced under low temperature appeared to have a superior agronomic significance. On the other hand, the sulphur content was low at 500 °C pyrolysis temperature followed by 400 °C and high at 600 °C. At 600 °C the highest sulphur content was recorded by MSB (0.091) followed by BGB (0.084), PNB (0.062) and lowest for LCB (0.009).

3.8. Carbon dynamics

With increase in charring temperature the C:N ration of the four different biochar increased significantly (Table 3). The highest C:N ration was recorded by PNB (105) biochar followed by LCB (99), MSB (87) and lowest for BGB (79). The application of such high C:N ratio biochar in soil would enhance to immobilize the soil available nitrogen followed by its deficiency via microbial nitrogen assimilation to break down highly recalcitrant biochar substrate and such situation will temporarily affect the available soil nutrients for plants growth (Stevenson 1994). But, as huge amount of biochar carbon is aromatic and condensed its degradation is very difficult by soil microbes and thus doubtfully biochar would cause major nitrogen immobilization. Thus, to get maximum benefit of biochar soil scientists always suggests that biochar should be applied in soil along with inorganic or organic fertilizers (Carrier et al., 2012). Biochar produced from high carbon containing (wood) feedstocks had a lower ash substances and higher C:N ratio than biochar prepared from low carbon biomass like grass, weeds and manure (Mukome et al., 2013). The dissolved organic carbon content (DOC) and index for microbial C-use efficiency of biochar decreased significantly with increase in pyrolysis temperature. They were low at 600 °C pyrolysis temperature followed by 500 °C and high at 400 °C. The highest DOC was recorded by BGB (0.79) followed by MSB (0.75), PNB (0.67) and lowest for LCB (0.61). The biochar DOC is very important parameter for assessing the soil organic carbon dynamics and played a critical role in transport of contaminants in soil. Without a doubt, the quantity of biochar DOC reduced exponentially with augmentation in pyrolysis temperature and it was due to enhanced carbonization process at higher pyrolysis temperature. Additionally, tree and weed feedstock derived biochar (PNB and LCB) generated small quantity of DOC as compare to crop feedstock derived biochar (MSB and BGB). The tree and weed feedstocks usually contain huge lignin as compared with crop feedstocks (less lignin) and lignin is more stable thermally than hemicellulose and cellulose. Therefore, high lignin content feedstocks are more able to form solid biochar rather than liquid bio-oil and thus produced lower amount of DOC from tree and weed biochar. If biochar is considered for soil carbon sequestration then it is desirable that it should have minimum very labile DOC fractions and maximum stable carbon. But interestingly, if biochar is considered for soil aggregation and structure improvement, microbe's food source for increasing soil nutrients availability, water holding capacity and biochar based controlled release fertilizers, it is essential to release small quantity of very labile DOC fractions (Liu et al., 2019). The highest index for microbial carbon use efficiency content was recorded by LCB (0.916) followed by PNB (0.856), MSB (0.537) and lowest for BGB (0.437) and its value decreased with increase in temperature. The decrease in the index for microbial carbon use efficiency may be attributed to the decreased dissolved organic carbon and increased C:N ration with increase in charring temperature. High temperature derived biochar show high C:N ration resulting more stable (immobilization) carbon and thus microbes are unable to utilize the carbon and thereby decreased use efficiency.

3.9. Principal component analysis

At varying pyrolysis temperature, bivariate Pearson correlation coefficients between the biochar parameters were analyzed and based on the correlation co-efficient (r) values their association has been evaluated. In principal component analysis, variables were scaled/standardized in the context of data analysis before PCA and clustering analysis. Only the PCs with eigen values ≥ 1 were examined. Fig. 5 (A-a) showed the distance between variables and the origin, measures the quality of the variables. Variables which were positively correlated are grouped together whereas negatively correlated variables are positioned on opposite sides of the plot origin. The BET, TPV, MPV and MC were highly positively correlated among themselves and thus forming one cluster. Similarly, WHC and APD formed second cluster; BD and PO third cluster and variable Y showed very low (positive/negative) correlation with all the variables. Fig. 5 (AB-a) showed that the PCA has identified four PCs with eigen values > 1.0, altogether accounted for a variation of 93.73% of the total variation present in the original dataset. Fig. 5 (AB-b) represented that S, CEC, EA and SNC were positively correlated among themselves and thus forming one cluster. The pHs, pHw, CCE and B formed second cluster based on their similarity. Fig. 5 (AB-b) showed that for biochar chemical properties the PCA identified two PCs with eigen values > 1.0, altogether accounted 75.97% variation of the total variation present in the original dataset. Fig. 5 (AB-c) showed that the Vm, TO and DOC were positively correlated among themselves and thus formed one cluster. The TN, TH, ASh and S formed second cluster based on their similarity; and C:N, FCc, TC, and CUE formed third cluster. Fig. 5 (AB-c) showed that for ultimate, proximate & carbon properties of biochar the PCA identified three PCs with eigen values > 1.0, altogether

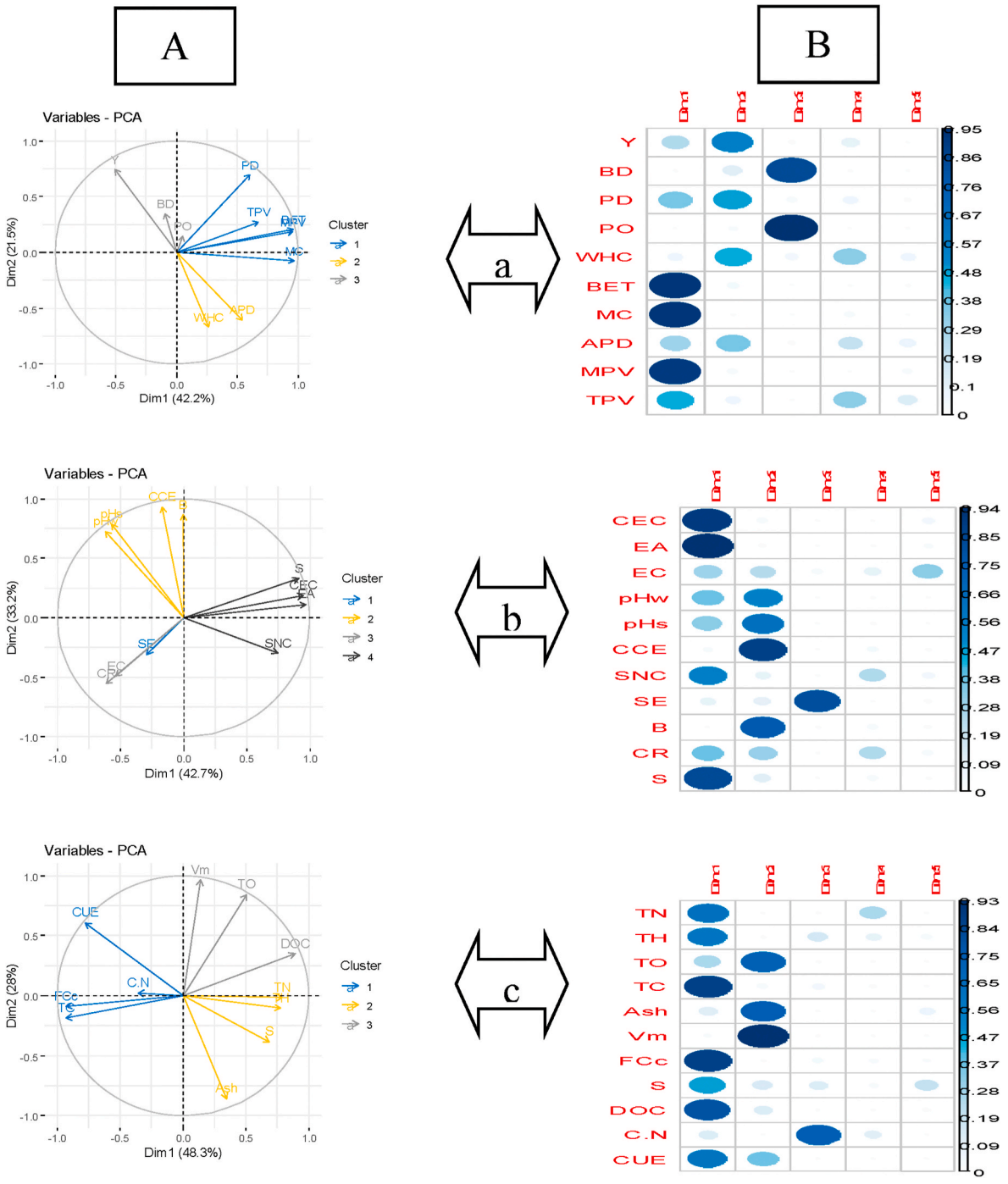

Fig. 5. Principal component analysis: (A) factor map & clustering of variables and (B) quality of representation of the variables in a given principal components for (a) physical properties (b) chemical properties (c) ultimate-, proximate analysis & carbon of different feedstock derived biochar produced at different pyrolysis temperature.

accounted 86.56% variation of the total variation present in the original dataset.

4. Conclusion

In conclusion the pyrolysis temperature notably influenced all the functionalities of biochar. The produced biochar can replace the conventional fossil fuels due to their high fixed carbon. Additionally, for developing various carbon materials the biochar may serve as a carbon source. The different pyrolysis, carbonization, and gasification procedure (thermal degradation) might help to decrease the pollution and deforestation, at the same time supplying huge quantity of chemical resource and renewable fuel. The highly porous biochar can be used as a biosorbent, soil amendments or biofertilizer as it contained more average diameter, micro pore volume and total pore volume along with plentiful in plant available nutrients as well as functional groups. The resulted biochar with higher porosity and BET surface area might have some positive effect on structural modification of soil and nutrient retention which can offer improved environment for beneficial soil microbiological growth and development. Certain biochar characteristics are largely depends on pyrolysis temperature and some characteristics are largely controlled by feedstock types and thus its applications

requiring these properties would call for a better attention and awareness to the choice of feedstocks. During designing a specialized biochar for using in any contexts, pyrolysis temperature and feedstocks are the main factors to be considered that manipulates the real value of biochar for its application.

CRediT author statement

Shaon Kumar Das: Complete research work, data interpretation and article writing. Goutam Kumar Ghosh: Research work monitoring, editing manuscript and review. Ravikant Avasthe: Research work monitoring, editing manuscript and review. Kanchan Sinha: Statistical analysis

Declaration of competing interest

The authors declare that they have no known competing financial interests or personal relationships that could have appeared to influence the work reported in this paper.

Acknowledgements

The first author (Shaon Kumar Das) is thankful to the Director, ICAR Research Complex for NEH Region, Umiam, Meghalaya, India and Department of Soil Science and Agricultural Chemistry, Palli Siksha Bhavana, Visva Bharati, Shantiniketan, West Bengal, India for providing financial and research work facility during the entire period of study.

References

Al-Wabel, M.I., Hussain, Q., Usman, A.R.A., Ahmad, M., Abduljabbar, A., Sallam, A.S., Ok, Y.S., 2017. Impact of biochar properties on soil conditions and agricultural sustainability: a review. Land Degrad. Dev. 29 (7), 2124–2161.

AOAC, 1999. Official Methods of Analysis of the Association of Official Analytical Chemists, sixteenth ed. Association of Official Analytical Chemists, Arlington, VA.

ASTM-E 1755, 1995. Ash in Biomass. Annual Book of ASTM standards.

ASTM-E 872, 1982. Volatile Matter in the Analysis of Particulate Wood Fuels. Annual Book of ASTM standards.

Berger, K.C., Truog, E., 1939. Boron determinations in soils and plants. Industrial and engineering chemistry. Analytical edition 11, 540–545.

Cantrell, K.B., Hunt, P.G., Uchimiya, M., Novak, J.M., Ro, K.S., 2012. Impact of pyrolysis temperature and manure source on physicochemical characteristics of biochar. Bioresour. Technol. 107, 419e428.

Cao, X., Harris, W., 2010. Properties of dairy-manure-derived biochar pertinent to its potential use in remediation. Bioresour. Technol. 101 (14), 5222–5228.

Case, S.D.C., Mcnamara, N.P., Reay, D.S., Whitaker, J., 2014. Can biochar reduce soil greenhouse gas emissions from a Miscanthus bioenergy crop? GCB Bioenergy 6, 76e89.

Cely, P., Gascó, G., Paz-Ferreiro, J., Méndez, A., 2015. Agronomic properties of biochars from different manure wastes. J. Anal. Appl. Pyrol. 111, 173–182.

Chapman, H.D., 1965. Cation exchange capacity. In: Black, C.A. (Ed.), Methods of Soil Analysis. American Society of Agronomy, Madison, pp. 891–901.

Das, S.K., Avasthe, R.K., Singh, M., 2016. Carbon negative biochar from weed biomass for agricultural research in India. Curr. Sci. 110 (11), 2045–2046.

Dias, B., Silva, C., Higashikawa, F., Roig, A., Sanchez-Monedero, M., 2010. Use of biochar as bulking agent for the composting of poultry manure: effect on organic matter degradation and humification. Bioresour. Technol. 10, 1239–1246.

Farina, M.P.W., Channon, P., 1991. A field comparison of lime requirement indices for maize. Plant Soil 134, 127–135.

Fidel, R.B., Laird, D., Thompson, A.M.L., 2013. Evaluation of modified Boehm titration methods for use with biochars. J. Environ. Qual. 42, 1771–1778.

Gai, X., Wang, H., Liu, J., Zhai, L., Liu, S., Ren, T., Liu, H., 2014. Effects of feedstock and pyrolysis temperature on biochar adsorption of ammonium and nitrate. PloS One 9, e113888.

Hassnen, J., Zaid, H.M., Anmar, D., 2020. Incorporating of two waste materials for the use in fine grained soil stabilization. Civ. Eng. J 6 (6), 1114–1123.

Hernandez-Mena, L., Pecora, A., Beraldo, A., 2014. Slow pyrolysis of bamboo biomass: analysis of biochar properties. Chemical Engineering Transactions 37, 115–120.

Jackson, M.L., 1973. Soil Chemical Analysis. Prentice Hall of India Pvt. Ltd., New Delhi, p. 498.

Jankowska, H., Swiatkowski, A., Choma, J., 1991. Active Carbon. Ellis Horwood, New York.

Karim, A.A., Kumar, M., Mohapatra, S., Singh, S.K., 2019. Nutrient rich biomass and effluent sludge wastes co-utilization for production of biochar fertilizer through different thermal treatments. J. Clean. Prod. https://doi.org/10.1016/j.jclepro.2019.04.330.

Kavitha, B., Reddy, P.V.L., Kim, B., Lee, S.S., Pandey, S.K., Kim, K.H., 2018. Benefits and limitations of biochar amendment in agricultural soils: a review. J. Environ. Manag. 227, 146–154.

Khanmohammadi, Z., Afyuni, M., Mosaddeghi, M.R., 2015. Effect of pyrolysis temperature on chemical and physical properties of sewage sludge biochar. Waste Manag. Res. 33, 275e283.

Lehmann, J., Joseph, S.M., 2015. Biochar for Environmental Management: Science and Implemetation, second ed. Earthscan, London, p. 997.

Li, S., Chen, G., 2018. Thermogravimetric, thermochemical, and infrared spectral characterization of feedstocks and biochar derived at different pyrolysis temperatures. Waste Manag. 78, 198–207.

Liu, C.H., Chu, W., Li, H., Boyd, S.A., Teppen, B.J., Mao, J., Zhang, W., 2019. Quantification and characterization of dissolved organic carbon from biochars. Geoderma 335, 161–169.

Masoumeh, H., Hamed, M.Z., Peyman, D.A., Mehdi, Z., 2019. Economic and environmental impacts of cropping pattern elements using systems dynamics. Civ. Eng. J 5 (5), 1020–1032.

Muhammad, J.M., Abdul, R.M., 2020. Wheat straw optimization via its efficient pretreatment for improved biogas production. Civ. Eng. J 6 (6), 1056–1063.

Mukherjee, A., Zimmerman, A.R., 2013. Organic carbon and nutrient release from a range of laboratory-produced biochars and biochar-soil mixtures. Geoderma 193, 122–130.

Mukome, F.N.D., Zhang, X., Silva, L.C.R., Six, J., Parikh, S.J., 2013. Use of chemical and physical characteristics to investigate trends in biochar feedstocks. J. Agric. Food Chem. 61, 2196–2204.

Novak, J., Ro, K., Ok, Y.S., Sigua, G., Spokas, K., Uchimiya, S., Bolan, N., 2016. Biochars multifunctional role as a novel technology in the agricultural, environmental, and industrial sectors. Chemosphere 142, 1–3.

Prost, K., Borchard, N., Siemens, J., Kautz, T., Séquaris, J., Amelung, W., 2012. Biochar affected by composting with farmyard manure. J. Environ. Qual. 42 (1), 164–172.

Ronsse, F., van Hecke, S., Dickinson, D., Prins, W., 2013. Production and characterization of slow pyrolysis biochar: influence of feedstock type and pyrolysis conditions. GCB Bioenergy 5 (2), 104–115.

Stevenson, F.J., 1994. Humus Chemistry: Genesis, Composition, Reactions. John Wiley & Sons, New York, USA.

Subbiah, B.V., Asija, G.L., 1956. A rapid procedure for the determination of available nitrogen in soil. Curr. Sci. 25, 259–260.

Veihmeyer, F.J., Hendrickson, A.H., 1948. The permanent wilting percentage as a reference for the measurement of soil moisture. Trans. Am. Geophys. Union 29. https://doi.org/10.1029/TR029i006p00887,issn:0002-8606.

Wang, M., Zhu, Y., Cheng, L., Andserson, B., Zhao, X., Wang, D., Ding, A., 2018. Review on utilization of biochar for metal-contaminated soil and sediment remediation. J. Environ. Sci. (China) 63 (1), 156–173.

Yargicoglu, E.N., Sadasivam, B.Y., Reddy, K.R., Spokas, K., 2015. Physical and chemical characterization of waste wood derived biochars. Waste Manag. 36, 256–268.

Yuan, H., Lu, T., Huang, H., Zhao, D., Kobayashi, N., Chen, Y., 2015. Influence of pyrolysis temperature on physical and chemical properties of biochar made from sewage sludge. J. Anal. Appl. Pyrol. 112, 284e289.

Zhang, A., Cheng, G., Hussain, Q., Zhang, M., Feng, H., Dyck, M., Wang, X., 2017. Contrasting effects of straw and straw–derived biochar application on net global warming potential in the Loess Plateau of China. Field Crop. Res. 205, 45–54.

Zhao, L., Cao, X., Masek, O., Zimmerman, A., 2013. Heterogeneity of biochar properties as a function of feedstock sources and production temperatures. J. Hazard Mater. 256–257, 1–9.